Check for updates

Fish and Fisheries

WILEY

FISH and FISHERIES

ORIGINAL ARTICLE OPEN ACCESS

Offspring Size Resolves a Population Growth Paradox in Rays and Skates

Ellen Barrowclift[1] | Jennifer S. Bigman[2] | Eric D. Digel[3] | Per Berggren[1] | Nicholas K. Dulvy[3]

[1]School of Natural and Environmental Sciences, Newcastle University, Newcastle-upon-Tyne, UK | [2]School of Marine Science and Policy, University of Delaware, Lewes, Delaware, USA | [3]Earth to Ocean Research Group, Department of Biological Sciences, Simon Fraser University, Burnaby, British Columbia, Canada

Correspondence: Per Berggren (per.berggren@newcastle.ac.uk)

Received: 11 September 2025 | **Revised:** 14 April 2026 | **Accepted:** 16 April 2026

Keywords: biogeography | chondrichthyes | data-poor fisheries | life history theory | risk assessment | temperature-size rule

ABSTRACT

The maximum intrinsic population growth rate, r_{max}, is a key determinant of sustainable fishing limits and is increasingly used in risk assessments. We previously showed how the r_{max} of rays and skates (subclass Batoidea) scales with adult body size, temperature (and hence depth) such that smaller-bodied species and those in warmer, shallower waters have greater r_{max} and, therefore, will be less sensitive to overexploitation. Paradoxically however, warm shallow-water tropical rays have lower r_{max} than cold deepwater temperate skates, *contra* to the expectation from metabolic scaling theory. To resolve this paradox, we examine how r_{max} is related to adult and offspring size (while accounting for temperature and depth) across 85 ray and skate species. Offspring size mediates relationships between r_{max}, adult body size, temperature and depth. Despite inhabiting warmer, shallower waters, tropical rays generally have larger offspring and lower r_{max} compared to temperate skates. Our result explains why tropical rays are less resilient to overfishing despite expectations from metabolic theory that tropical species should have faster life histories and therefore higher r_{max} and greater resilience than temperate species. Although the drivers of large offspring size in tropical rays remain uncertain, we use basic models of temperature- and size-dependent predation to hypothesise that this is due to greater predation risk in shallow tropical waters selecting for increased maternal investment in offspring size via evolution in viviparity and matrotrophy. Our work highlights the complex relationships among life histories and the environment and may help explain global biogeographic patterns of intrinsic sensitivity to exploitation.

1 | Introduction

A key challenge in population biology is understanding global patterns of life histories, which is of both fundamental interest as well as useful for identifying species sensitivity to overfishing and other anthropogenic threats. Biogeographic patterns in life histories appear to be mediated by temperature (Beukhof et al. 2019). Further, the temperature-size rule (TSR) describes the observed pattern that ectothermic populations and species generally grow faster to a smaller size at maturity (and presumably, smaller adult size) in warmer temperatures (Atkinson 1994; Atkinson and Sibly 1997; Atkinson et al. 2006). Finally, metabolic theory suggests that species in warmer waters (e.g., in the shallow waters of the tropics) with higher metabolic rates will tend to have 'faster' life histories than those in cooler waters (e.g., high latitude and deep waters) (Juan-Jordá et al. 2013; Beukhof et al. 2019; Wong et al. 2021; Gravel et al. 2024). Typically, species with faster life histories grow faster to a smaller maximum body size, mature earlier and have shorter lifespans, resulting in higher maximum intrinsic rate of population increase, r_{max} (Hutchings et al. 2012; Thorson 2020; Gravel et al. 2024).

r_{max} is the average annual number of female spawners produced per female spawner at low population density (i.e., in the absence

This is an open access article under the terms of the Creative Commons Attribution License, which permits use, distribution and reproduction in any medium, provided the original work is properly cited.

© 2026 The Author(s). *Fish and Fisheries* published by John Wiley & Sons Ltd.

of density-dependence) and is the equivalent of the fishing mortality capable of driving the species or population to extinction ($F_{extinct}$) (Dulvy et al. 2004). Hence, r_{max} is an essential component of fisheries management to determine fishing limits and species' recovery potentials (Myers and Worm 2005; Worm et al. 2013; Cortés 2016; Pardo et al. 2016; Horswill et al. 2025; Dulvy et al. 2026). There is considerable interest in calculating r_{max} for chondrichthyans but general patterns have proven hard to find (Mejía et al. 2025) unless trait data are carefully matched from similar habitats and consistent models are used (Pardo and Dulvy 2022; Gravel et al. 2024; Moro et al. 2025). According to metabolic scaling expectations, r_{max} scales negatively with (adult) body mass (with an exponent of −0.25) and, independently, increases with temperature according to an Arrhenius process (Brown et al. 2004; Savage et al. 2004). This size- and temperature-dependent scaling has been shown empirically both in experimentally-manipulated populations as well as across species in the wild (Luhring and Delong 2017; Bernhardt et al. 2018). For example, a positive relationship between r_{max} and temperature exists across Atlantic cod (*Gadus morhua*, Gadidae), which has greater r_{max} in warmer, more southerly populations (Myers et al. 1997; Savage et al. 2004). These differences in r_{max} have consequences for how populations respond to anthropogenic mortality such as from fishing. For example, after controlling for fishing mortality, cooler, temperate tunas (Scombridae) with slower life histories experienced greater population declines than tropical lower-latitude tunas with faster life histories (Juan-Jordá et al. 2011, 2015). More generally, size-based modelling has shown the ratio of production to biomass (P:B), mediated by temperature, changes systematically with latitude across the world's fish communities, with high production and low standing biomass in the tropics compared to that found at cooler temperate and polar latitudes (Jennings et al. 2008).

Our previous work revealed a positive relationship between r_{max} and temperature across skates and rays consistent with metabolic theory, but we found that warm, shallow-water rays had lower r_{max} than cold, deep-water skates but could only speculate at the reasons (Barrowclift et al. 2023). Since then, recent work suggests that in addition to temperature and adult size, offspring size may also be an important determinant of r_{max}, as two species with the same adult mass may differ in the number and size of offspring produced, and consequently have different maximum population growth rates (Neuheimer et al. 2015; Denéchère et al. 2022). This suggests that for two species with the same adult mass, one with larger offspring (and fewer of them) may have a lower r_{max} and therefore, offspring size could affect the scaling of r_{max} (Burger et al. 2019; Denéchère et al. 2022). We are now able to test whether offspring size can explain the paradox revealed by our earlier work (Barrowclift et al. 2023).

Rays and skates of the superorder Batoidea are widely distributed across the world's oceans with a distinct biogeographic separation. Skates generally have an anti-tropical distribution and are typically found in the cooler waters of polar and temperate seas, as well as deeper, cool waters in the tropics (McEachran and Miyake 1990; Ebert and Compagno 2007; Frisk 2010). Whereas rays are generally found in the shallow tropics, subtropics and with seasonal occurrence in temperate waters during summer. Most rays are live-bearers with very low fecundity and generally have larger offspring compared to skates, which lay numerous eggs (mermaid's purses) and overall have smaller offspring (Goodwin et al. 2002; Mull et al. 2024). Here, we build on our recent study that showed how temperature (and depth) and body size correlate to r_{max} in batoids (Barrowclift et al. 2023) by testing whether the larger offspring size of tropical rays explains the paradox of their lower r_{max} compared to skates, while accounting for these known important covariates for 85 batoid species.

2 | Material and Methods

We first describe the mapping of batoid species richness. Second, we present the calculation of r_{max}, including the sources of the life history data used in the calculations. Third, we describe the calculation of environmental temperature-at-depth. Fourth, we summarise our analytical approach, including the statistical models used to assess different hypotheses of how r_{max} may vary with adult and offspring mass, temperature and depth. Finally, we develop a basic model of temperature-dependent metabolic- and size-based mortality that might influence cohort sizes for ray and skate offspring sizes.

2.1 | Mapping of Ray and Skate Richness

We downloaded species distribution maps from the IUCN Red List as shapefiles (https://www.iucnredlist.org/resources/spatial-data-download). These were mapped to a hexagonal grid with cell sizes averaging 23,322 km^2 and species richness was calculated per cell for each of skate (Order Rajiformes) and ray species (Orders: Torpediniformes; Rhinopristiformes and Myliobatiformes) (Dulvy et al. 2014, 2021). Species richness was calculated for each hexagonal spatial grid cell and plotted against latitude after removing zero and non-finite values. Latitudes were grouped into 5° bands using floor-based binning. Individual grid cells are shown as points, coloured by richness using a reversed viridis gradient. The plot displays raw grid-cell values (not band means), with latitude ranging from 90° S to 90° N and richness constrained to 0–65 species. The lines are loess (locally weighted regression) fit to the upper 90th centile of the richness cells with a span of 0.4.

2.2 | The Calculation of r_{max} and Source of Life History Data

The maximum intrinsic rate of population increase, r_{max}, was calculated using a modified Euler-Lotka model, with a mortality estimator that accounts for survival to maturity with the following equation:

$$l_{\alpha_{mat}} b = e^{r_{max}\alpha_{mat}} - e^{-M}(e^{r_{max}})^{\alpha_{mat}-1}, \quad (1)$$

where $l_{\alpha_{mat}}$ is the proportion of individuals surviving to maturity, which is calculated from annual fecundity b and the species-specific instantaneous natural mortality rate M (Cortés 2016; Pardo et al. 2016). Natural mortality (M) was estimated as $M = 1/\omega$ (Dulvy et al. 2004) where ω is an estimate of average lifespan in years and was assumed to be the midpoint between age at maturity (α_{mat}) and maximum age (α_{max}) (Pardo et al. 2016). The life history traits were sourced for 85 ray (Torpedo rays,

14672979, 0, Downloaded from https://onlinelibrary.wiley.com/doi/10.1111/faf.70091 by Nick Dulvy , Wiley Online Library on [12/05/2026]. See the Terms and Conditions (https://onlinelibrary.wiley.com/terms-and-conditions) on Wiley Online Library for rules of use; OA articles are governed by the applicable Creative Commons License

Torpediniformes; Rhino rays, Rhinopristiformes; and stingrays, Myliobatiformes; $n = 53$) and skate species (Rajiformes; $n = 32$). Three traits were geographically matched where possible to minimise spurious errors due to intraspecific life history variation (Gravel et al. 2024; Moro et al. 2025): (1) female age at 50% maturity (α_{mat}; years), (2) maximum age for females, where known (α_{mat}; years) and (3) annual reproductive output (number of female offspring assuming 1:1 sex ratio; *b*) reported in a published global life history database (Barrowclift and Dulvy 2023) compiled in Barrowclift et al. (2023).

Adult body mass (maximum weight in grams) for the 85 batoid species was also sourced from the published life history database compiled in Barrowclift et al. (2023). Offspring mass (in grams) was estimated from offspring size measured as total length for skates or disc width for rays in centimetres (cm) as reported in Rays of the World (Last et al. 2016), Sharkipedia (Mull et al. 2022) and IUCN Red List assessments (Dulvy et al. 2021). Offspring size was not available for 14 species and for these cases we estimated offspring size from related species with similar maximum length and body shape (Barrowclift and Dulvy 2023). The median offspring length was calculated in cases when minimum and maximum offspring lengths were reported. The corresponding offspring mass was then calculated using length-weight regression coefficients extracted from FishBase using the package *rfishbase* (Boettiger et al. 2012; Froese and Pauly 2022; Barrowclift and Dulvy 2023). Length-weight regression coefficients were selected for females where possible. When length-weight regressions were not available, we used parameters for a closely related species with similar body shape and maximum size (Barrowclift and Dulvy 2023).

2.3 | Calculation of Environmental Temperature-At-Depth

Median depth and environmental temperature for the 85 ray and skate species were also taken from Barrowclift et al. (2023). Specifically, median depth estimates for each species were taken from depth ranges of IUCN Red List assessments as compiled in Dulvy et al. (2021). Temperature-at-depth data were determined by intersecting each species distribution map with the International Pacific Research Center's interpolated dataset of gridded mean annual ocean temperatures. This dataset is based on measurements from the Argo Project (data available at http://apdrc.soest.hawaii.edu/projects/Argo/data/statistics/On_standard_levels/Ensemble_mean/1x1/m00/index.html) and is comprised of water column temperatures, which include seafloor temperatures. Species range maps were sourced from https://www.iucnredlist.org/resources/spatial-data-download. Temperature grid points were extracted across the species' distribution from the depth level that was closest to the species' median depth and the median temperature calculated (Pardo and Dulvy 2022; Barrowclift et al. 2023).

2.4 | Statistical Inference

Metabolic scaling expectations for how r_{max} relates to adult body mass and temperature (Savage et al. 2004) can be estimated with the following linear model:

$$\ln(r_{max}) = \beta_0 + \beta_1 * \ln(M) + \beta_2 * 1/k_B T, \quad (2)$$

where r_{max} is the maximum intrinsic rate of population increase (year^{-1}), β_0 is the intercept, β_1 is the body mass-scaling coefficient, M is adult mass in grams, β_2 is the activation energy E in electron volts (eV), T is the absolute temperature (in Kelvin, K) and k_B is the Boltzmann constant (8.617×10^{-5} eV).

We modified this initial Equation (2) above to test whether absolute offspring size ($M_{offspring}$) and the adult to offspring mass ratio ($M/M_{offspring}$) explained variation in r_{max} across species in addition to temperature and depth (Denéchère et al. 2022). The tested hypotheses and corresponding models are outlined in table 1. $M/M_{offspring}$ was suggested by Denéchère et al. (2022) to be a better predictor of r_{max} than either adult or offspring body mass and thus it is examined here. Specifically, we used an information-theoretic approach to compare a total of 32 models that represented different hypotheses as to how r_{max} may vary across species (see Table S1 for hypotheses, models and AIC values and weights).

For model fitting, r_{max}, adult and offspring masses were natural log-transformed, and temperature and depth data were standardised (scaled and centred). We found that offspring body mass and adult body mass as well as temperature and depth were collinear (Pearson's $r > 0.75$), but there was no relationship between either adult or offspring body mass and temperature. Thus, we only included either offspring body mass or adult body mass and either temperature or depth in a given model, and did not consider interactions between either mass and either temperature or depth. All models were run in a phylogenetic comparative framework to account for the shared evolutionary history between species. To do so, we fit phylogenetic generalised linear models (pgls) using the *pgls* function in the *caper* package (Orme et al. 2018), with Pagel's λ estimated by maximum likelihood. Model assumptions were validated prior to each candidate model being used for hypothesis testing. Variance-inflation factors (VIF) were estimated to assess collinearities for all coefficients in the models using the car package (Fox and Weisberg 2019); no VIF value was greater than two, except as expected when interactions were included, indicating that models were robust to collinearity. The residuals of each pgls model were visually inspected against fitted values to check for homoscedasticity, and the normality of residuals was assessed using quantile-quantile plots. Additionally, the strength of the phylogenetic signal was evaluated by estimating and profiling Pagel's λ for each pgls model.

Phylogeny was used as a random effect in all models using a phylogenetic tree randomly drawn from the distribution of chondrichthyan trees (Stein et al. 2018) (available at Vertlife.org). The binomial nomenclature of the trees was updated to reflect current taxonomic nomenclature. The phylogenetic position of two species was not known (*Aetobatus narutobiei*, Aetobatidae and *Maculabatis ambigua*, Dasyatidae), and therefore, two closely related species (*A. flagellum* and *M. gerrardi*, respectively) were used instead. Models were refitted with an additional 10 random trees to test the sensitivity of results to slight variations in the phylogenies used; the model rankings remained consistent with temperature and depth interchangeable in the top model

14672979, 0, Downloaded from https://onlinelibrary.wiley.com/doi/10.1111/faf.70091 by Nick Dulvy , Wiley Online Library on [12/05/2026]. See the Terms and Conditions (https://onlinelibrary.wiley.com/terms-and-conditions) on Wiley Online Library for rules of use; OA articles are governed by the applicable Creative Commons License

(i.e., there was no practical effect of alternate phylogenetic hypotheses), and therefore, results were reported for a single tree (Table S2). The corrected Akaike Information Criterion (AICc) were used to compare models. If including a parameter improved the model's AICc by <2 units (ΔAICc ≤ 2), it was considered relatively uninformative (Burnham and Anderson 2002; Arnold 2010). All analyses were run in R version 4.1.2 (R Core Team 2021) in RStudio (RStudio Team 2021).

2.5 | Modelling Approach to Explore Intrinsic (Metabolic) and Extrinsic (Predation) Mortality Effects on Cohort Survival and Total Mortality

2.5.1 | Intrinsic (Metabolic) Mortality

We modelled intrinsic mortality according to metabolic scaling, assuming an Arrhenius temperature dependence and a quarter-power body-mass scaling. Intrinsic mortality ($\mu_{\text{intrinsic}}$; yr.$^{-1}$) was specified as $\mu_{\text{intrinsic}} \propto B_m^{(-1/4)\exp(-E/kT)}$, where B_m is body mass (kg), T is absolute temperature (K), E is activation energy (0.65 eV) and k is the Boltzmann constant (8.62×10^{-5} eV K^{-1}). To express $\mu_{\text{intrinsic}}$ in absolute units, we calibrated the proportionality constant such that $\mu_{\text{intrinsic}}$ at $B_m = 0.1$ kg (100 g) and $T = 15$°C equalled 0.3 yr.$^{-1}$.

2.5.2 | Extrinsic (Predation) Mortality

We explored two alternative representations of predation mortality ($\mu_{\text{predation}}$; yr.$^{-1}$): (i) a temperature-dependent (i.e., varying with latitude), size-independent model $\mu_{\text{predation}}(T) \propto \exp.(-E_{\text{predation}}/kT)$ ($E_{\text{predation}} = 0.50$ eV), calibrated so that $\mu_{\text{predation}}(15°C) = 0.20$ yr.$^{-1}$ under a 'medium predation' scenario; and (ii) a temperature-dependent, size-dependent model $\mu_{\text{predation}}(B_m) = \mu_{\text{ref}}\ (B_m/B_{m_\text{ref}})^{-b}$, with $B_{m_\text{ref}} = 0.1$ kg, $b = 0.35$, and $\mu_{\text{ref}} = 0.20$ yr.$^{-1}$ under the medium scenario. In both predation models we included three relative predation regimes (low/medium/high) implemented as multiplicative scalars (0.8, 1.0, 1.2) but only plotted the 'medium' scenario for clarity.

2.5.3 | Total Mortality and Cohort Survival

Total instantaneous mortality was computed additively as $\mu_{\text{total}} = \mu_{\text{intrinsic}} + \mu_{\text{predation}}$. We then explored the effect of total mortality on cohort survival for two offspring sizes. Cohort survival for an initial cohort of $N_0 = 1000$ individuals was modelled using exponential decay, $N(t) = N_0\ \exp.(-\mu_{\text{total}})$, over 0–10 years. We generated predictions across temperatures of 5°C, 15°C and 25°C and for two offspring sizes representing contrasting reproductive strategies (skate = 0.1 kg and ray = 1.0 kg), which will be differentially affected by size-based predation.

3 | Results

Globally, rays have higher species richness in the tropics, whilst skates are generally distributed in polar and temperate seas as well as deeper, cool tropical waters (Figure 1a,b). This is more apparent in latitudinal richness, with skates exhibiting a bimodal distribution with richness greatest in the mid-latitudes around 40°S and 40°N, whereas ray richness is unimodal, peaking in the tropics between 20°S and 30°N (Figure 1c,d; Figure S1). As with any biogeographical pattern there are a few exceptions of shallow-water tropical skates (e.g., Teevan's Skate *Dipturus teevani* and Rosette Skate *Leucoraja garmani*, Rajidae) as well as some deepwater ray exceptions (e.g., Deepwater Stingray *Plesiobatis daviesi*, Plesiobatidae and Sixgill Stingray *Hexatrygon bickelli*, Hexatrygonidae) (McEachran and

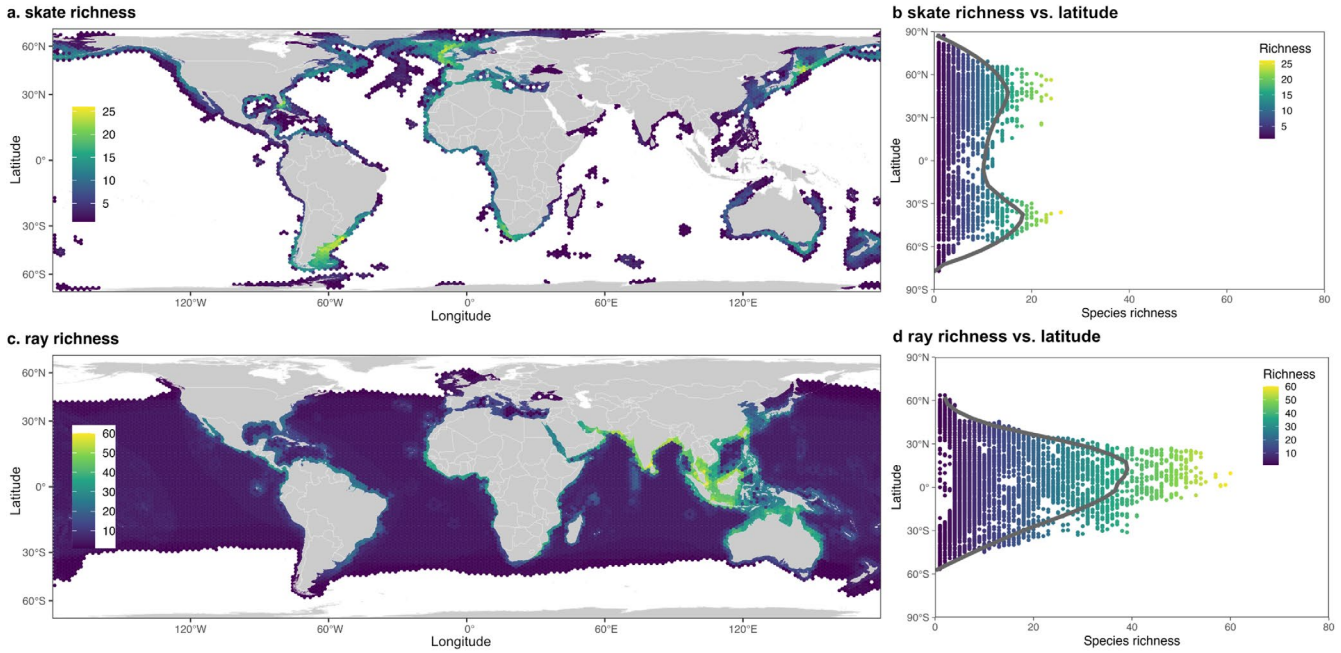

FIGURE 1 | (a, c) Biogeographic differences in the species richness of skates (a: $n = 284$ species of Rajiformes), which have a bimodal anti-tropical distribution, compared to rays, which have greater unimodal richness in the tropics (c: $n = 339$ species of Torpediniformes, Rhinopristiformes and Myliobatiformes), mapped to a hexagonal grid with cell size of ~23,322 km^2. (b, d) species richness with latitude for skates (b) and rays (d).

14672979, 0, Downloaded from https://onlinelibrary.wiley.com/doi/10.1111/faf.70091 by Nick Dulvy , Wiley Online Library on [12/05/2026]. See the Terms and Conditions (https://onlinelibrary.wiley.com/terms-and-conditions) on Wiley Online Library for rules of use; OA articles are governed by the applicable Creative Commons License

Miyake 1990; Ebert and Compagno 2007; Frisk 2010). This strong biogeographic separation in distributions was evident in the negative temperature-at-depth relationship for the batoids analysed in this study (Figure 2; Figure S2). The mean (±standard deviation) temperature of rays was 21.1°C (±8.9°C) compared to the much colder average of 8.9°C (±5.6°C) for skates (Figure 2). Our data had some 'cold' rays, including the regional endothermic devil rays (*Mobula birostris* and *M. mobular*) as well as the Pacific Torpedo Ray (*Tetronarce californica*), Marbled Torpedo Ray (*T. marmorata*) and Wide Stingaree (*Urolophus expansus*; Figure 2a) and two 'hot' skates, Starry Skate (*Raja asterias*) and Clearnose Skate (*Raja eglanteria*; Figure 2b). While there is a clear pattern of greater r_{max} at warmer temperatures (Barrowclift et al. 2023), there remains additional variation to be explained next.

On average, there was a positive relationship between adult mass and the adult to offspring mass ratio such that, at a comparable adult size (around 10^4 g or 10 kg), skate offspring were 0.1% of the adult mass compared to rays which were ten times larger at 1% of adult mass (Figure 3). While there is overlap between rays and skates, offspring mass scales positively with adult mass and there is a clear and significant separation between both groups such that skates have smaller absolute offspring sizes (Figure 4a). As a result, there is clear separation of both groups along the fecundity-offspring size trade-off (Figure 4a). Rays generally had low fecundity as a result of having larger offspring compared to skates, which were more fecund with smaller offspring reflecting the different reproductive strategies employed by egg-laying in skates and live-bearing with maternal investment in rays (Figure 4b). There was no significant relationship between temperature and either adult or offspring body mass but there were clear differences in offspring mass between rays and skates (Figure 5a), despite no significant difference in adult mass with temperature (Figure 5b).

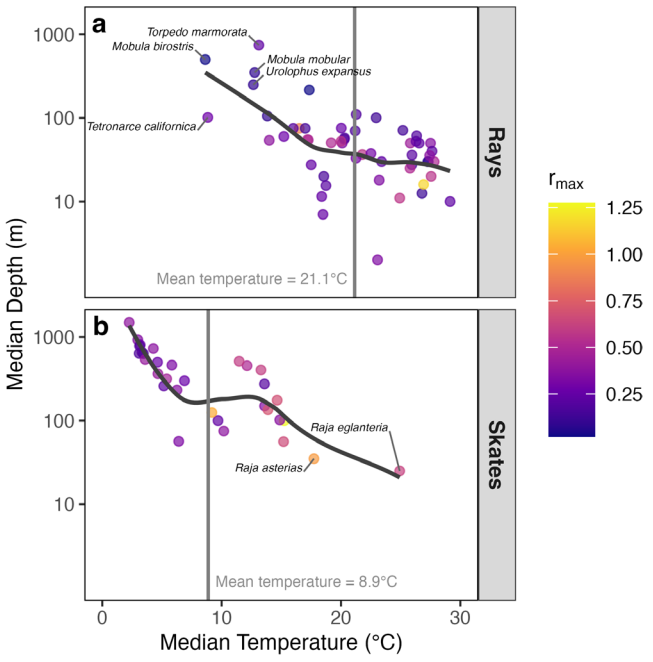

FIGURE 2 | Median temperature (°C) and depth (log10 m) distribution of maximum intrinsic rate of population increase (r_{max}) for (a) rays ($n = 53$) and (b) skates ($n = 32$). The cooler dwelling rays and warmer dwelling skates are labelled. The line is a loess (locally weighted regression) smooth with a span of 0.75.

Tropical rays had, on average, larger offspring and lower r_{max} compared to the temperate skates, despite living in warmer and shallower waters (Figures 6 and 7). We found that the ratio of adult to offspring size was not important in explaining variation in r_{max} and thus, we focus on the 11 models without this ratio in the main text (see Table S1 for results of the models with the adult to offspring size ratio). Our findings were insensitive to the exclusion of the two species with the largest offspring masses: *Mobula alfredi* and *M. birostris* (Mobulidae). The top models were the same; therefore, results were presented for the full 85 species dataset (Table S3).

Offspring size combined with either temperature or depth was the most important variable explaining the global variation in r_{max} across batoids (Figure 6). Of the 11 models examined, the most supported model suggests that r_{max} varies with offspring mass and depth (ΔAICc = 0), describing the greatest amount of variation in r_{max} across species (adjusted $R^2 = 0.20$; Table 1). The second-ranked model described r_{max} varying with offspring mass and temperature (ΔAICc = 0.3) and had approximately 86% of the support of the top-ranked model (when comparing the Akaike weights) and accounted for slightly less variation (adjusted $R^2 = 0.19$; Table 1). These top two models—one with depth and one with temperature—were essentially equivalent in terms of support, suggesting that either variable could be combined with offspring mass to explain the variation in r_{max} across rays and skates (Figures 6 and 7). Temperature and depth were interchangeable in the top model depending on the phylogeny (Table S2). In all models, the effect sizes of offspring mass, depth and temperature had 95% confidence intervals that did not overlap zero (Figure 6). A model describing r_{max} varying solely with offspring mass received 22% of the support of the top-ranked model and accounted for less variation (adjusted $R^2 = 0.16$). Therefore, including temperature or depth in the model with offspring mass improved the model support (based on AIC comparison; Table 1).

The effect of offspring mass on maximum population growth rate, r_{max}, of batoids is negative, indicating that r_{max} is lower in species with larger offspring sizes and higher in species with smaller offspring sizes (Figure 7; Table S4). Even after including offspring size in our models, r_{max} increases with temperature (and decreases with depth) in line with the expectation from metabolic theory (i.e., negative coefficient estimates for both inverse temperature $1/k_BT$ and depth across models) (Figure 7; Table S4). The relationship between temperature and r_{max} gave a coefficient estimate [β_2 in Equation (1)] of −0.44 (95% confidence intervals: −0.82 to −0.05; Table S4), which is broadly consistent with our original finding of metabolic theory prediction of approximately −0.6 to −1.0 (Figure 6) (Barrowclift et al. 2023). r_{max} was greater for species at shallower depths (Figure 7a) or at warmer temperatures (Figure 7b) based on the fitted top two models for the predicted relationships across three depths and three temperatures, respectively. Yet, overall tropical rays found in warmer, shallower waters had lower r_{max} than cool, deep-water skates due to their large offspring sizes.

14672979, 0, Downloaded from https://onlinelibrary.wiley.com/doi/10.1111/faf.70091 by Nick Dulvy , Wiley Online Library on [12/05/2026]. See the Terms and Conditions (https://onlinelibrary.wiley.com/terms-and-conditions) on Wiley Online Library for rules of use; OA articles are governed by the applicable Creative Commons License

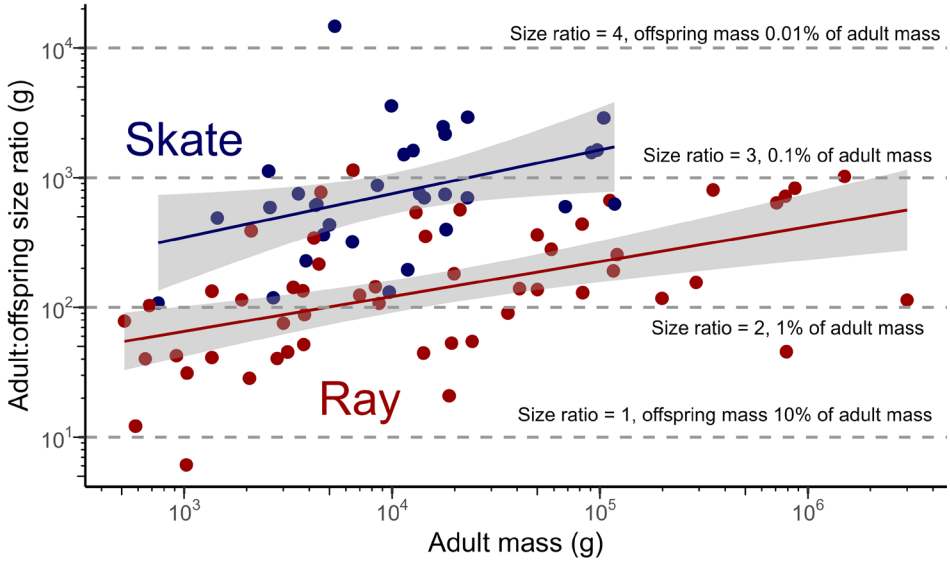

FIGURE 3 | Relationship between adult to offspring size ratio (g) and adult mass (g) in log10 space for 85 rays ($n = 53$, indicated by red points) and skates ($n = 32$, indicated by blue points). The grey bands around the fitted models show the confidence intervals and grey dashed lines show adult to offspring size ratios of 1 to 4 where offspring size is 10 to 0.01% of adult body mass, respectively.

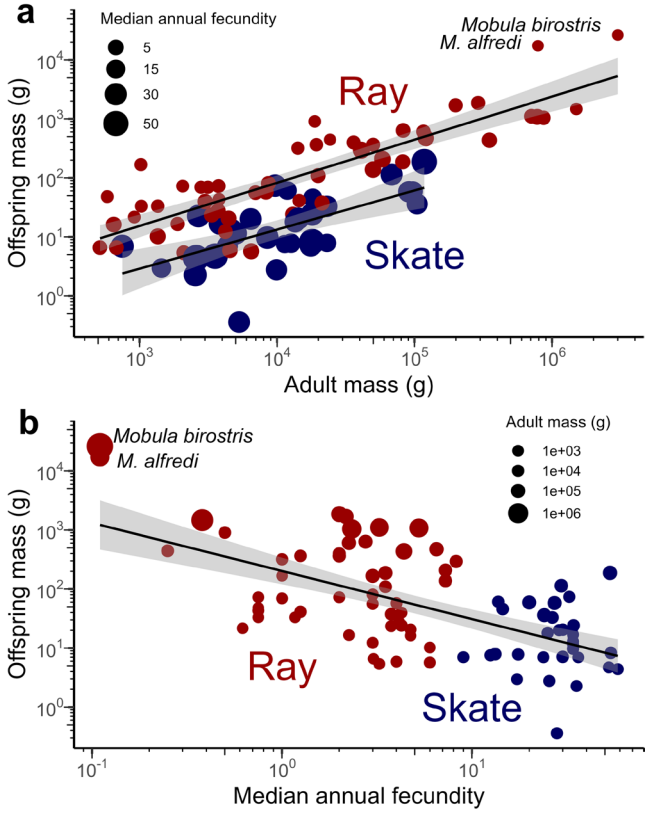

FIGURE 4 | Relationships between offspring body mass and (a) adult body mass (with point size showing median annual fecundity, that is, median number of female offspring per female per year) and (b) median annual fecundity (with point size showing adult mass) on a log10 scale for 53 rays (red points) and 32 skates (blue points).

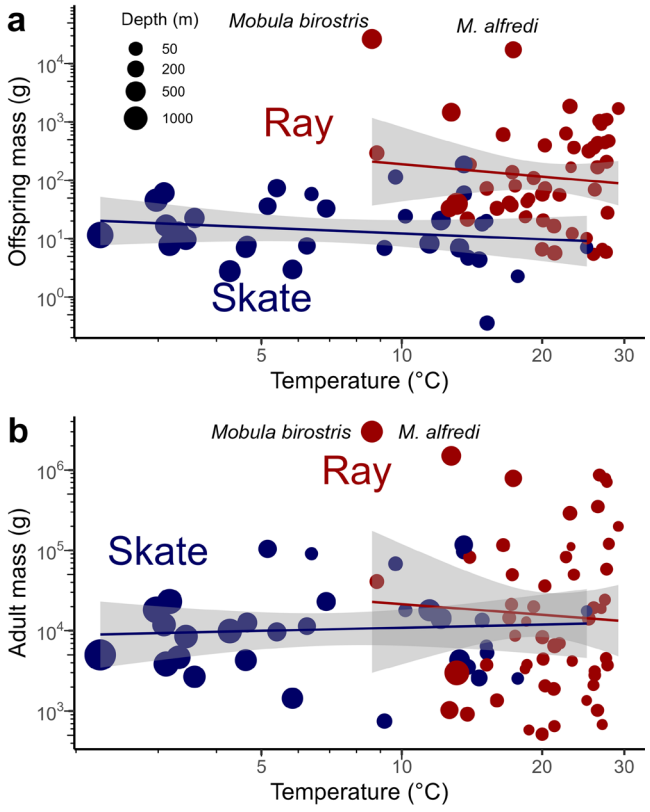

FIGURE 5 | Relationship between temperature (°C) and (a) offspring body mass (g) and (b) adult body mass (g) in log space for 85 rays ($n = 53$, indicated by red points) and skates ($n = 32$, indicated by blue points). Median depth of occurrence (m) is shown by the point size, with a linear model fitted to ray and skate data points. The grey bands around the fitted models show the confidence intervals.

By comparison, the remaining models were not well supported (ΔAICc > 6; Table 1). Adult mass did not have as much support as offspring mass in explaining variation in r_{max} across rays and skates. Models including offspring mass outperformed those including adult mass and models without any measure of size were far less supported than those with either offspring or adult

14672979, 0, Downloaded from https://onlinelibrary.wiley.com/doi/10.1111/faf.70091 by Nick Dulvy , Wiley Online Library on [12/05/2026]. See the Terms and Conditions (https://onlinelibrary.wiley.com/terms-and-conditions) on Wiley Online Library for rules of use; OA articles are governed by the applicable Creative Commons License

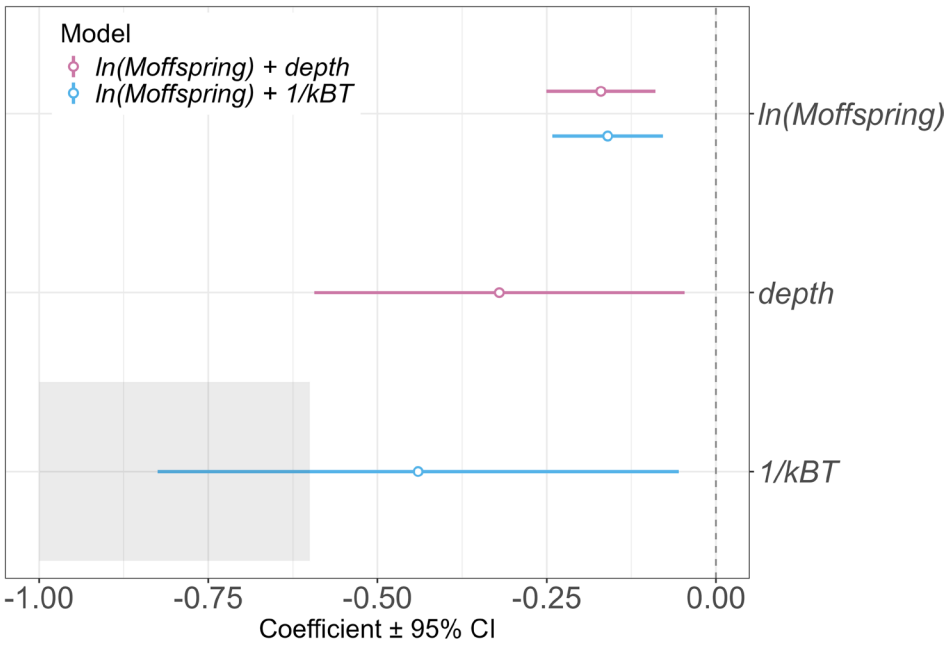

FIGURE 6 | Coefficient plot showing the effect sizes for offspring body mass ($M_{offspring}$), depth, and inverse temperature ($1/k_BT$) on r_{max} in the top two models. Error bars show the 95% confidence intervals (CI) and effect sizes are considered significant when confidence intervals do not overlap zero. The grey shaded box shows the expected effect size for temperature (−1.0 to −0.6) based on metabolic theory.

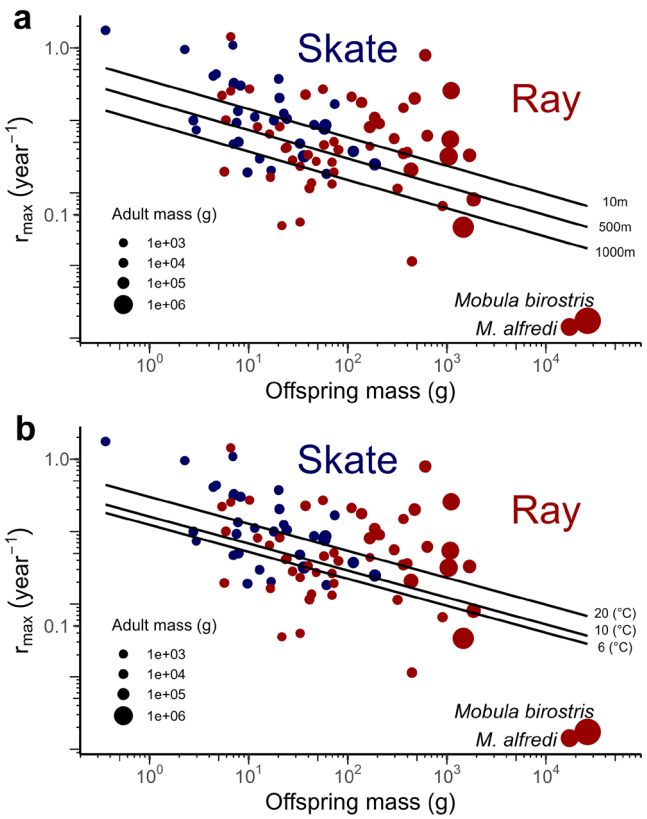

FIGURE 7 | Relationship between maximum intrinsic rate of population increase (r_{max}) and offspring body mass, showing the effects of either (a) depth or (b) environmental temperature for 85 rays ($n = 53$, red points) and skates ($n = 32$, blue points) in log10 space. Fitted lines show the predicted relationships for the two top models: (a) $\ln(r_{max}) \sim \ln(M_{offspring}) + \text{depth}$ for three depths (10, 500, 1000 m) and (b) $\ln(r_{max}) \sim \ln(M_{offspring}) + 1/k_BT$ for three temperatures (6°C, 10°C, 20°C). Adult body mass is shown by the point size.

size (Table 1). The top models (Rank 1 and 2 in Table 1) that included offspring mass were > 6 ΔAICc units better supported than the equivalent models with adult mass (model rank 4 and 5 in Table 1). Indeed, the effect of adult mass on r_{max} was approximately half (−0.12) that expected from metabolic theory (−0.25), with offspring mass having a larger negative effect size (coefficient estimate of −0.17; Table S4). These results indicate that increases in offspring size constrain r_{max} more strongly than increases in adult size.

For all models, there was a strong phylogenetic signal from the residuals of r_{max} with point estimates of Pagel's λ ranging between 0.79 and 0.92, albeit with wide confidence intervals (0.48–0.98; Table S4).

As specified by the Arrhenius approach, intrinsic (metabolic) mortality declined with increasing body mass, reflecting lower mass-specific metabolic rates in larger individuals. Predation mortality showed contrasting patterns in total mortality and cohort survival (Figure 8a,c vs. Figure 8b,d). Under the temperature-dependent model, predation mortality increased with temperature but remained independent of body size, leading to uniformly elevated total mortality across all masses at higher temperatures (Figure 8a; stepped green lines). In contrast, under the temperature-dependent + size-dependent predation model, predation mortality was highest in small individuals and declined with increasing body mass, resulting in strong early-life mortality bottlenecks (Figure 8b; negative green lines). Total mortality (Figure 8a,b; grey lines) integrated these intrinsic and extrinsic components, producing steep mortality gradients for small-bodied individuals, particularly at high temperatures and under size-dependent predation.

Cohort simulations revealed that these mortality patterns translated into marked differences in population persistence and

14672979, 0, Downloaded from https://onlinelibrary.wiley.com/doi/10.1111/faf.70091 by Nick Dulvy , Wiley Online Library on [12/05/2026]. See the Terms and Conditions (https://onlinelibrary.wiley.com/terms-and-conditions) on Wiley Online Library for rules of use; OA articles are governed by the applicable Creative Commons License

TABLE 1 | The 11 models examined with associated hypotheses for how maximum intrinsic rate of population increase (r_{max}) varies with offspring body mass ($M_{offspring}$), adult body mass (M), inverse temperature $1/k_BT$ and depth. Comparison of models using corrected Akaike Information Criteria (AICc), number of parameters (n), negative log-likelihood (−LL), adjusted R^2, difference in AICc from the top model (ΔAICc) and Akaike weights. Models are ordered by ascending AICc, with models with AICc < 2 shown in bold. The model specified includes * where an interaction term has been specified in the phylogenetic generalised linear models (pgls) model fitted.

Rank	Hypothesis	Model: $\ln(r_{max}) \sim$	n	-LL	AICc	R^2	Adj. R^2	ΔAICc	Weights
1	**r_{max} varies with offspring body mass and depth**	**$\ln(M_{offspring}) + \text{depth}$**	**3**	**−62.8**	**132**	**0.22**	**0.2**	**0**	**0.451**
2	**r_{max} varies with offspring body mass and temperature**	**$\ln(M_{offspring}) + 1/k_BT$**	**3**	**−63**	**132.3**	**0.21**	**0.19**	**0.3**	**0.388**
3	r_{max} varies with offspring body mass only	$\ln(M_{offspring})$	2	−65.4	135	0.17	0.16	3	0.101
4	r_{max} varies with adult body mass and temperature	$\ln(M) + 1/k_BT$	3	−66.1	138.5	0.14	0.12	6.5	0.017
5	r_{max} varies with adult body mass and depth	$\ln(M) + \text{depth}$	3	−66.1	138.6	0.14	0.12	6.6	0.017
6	r_{max} varies with adult body mass and temperature, and the effect of mass scaling coefficient varies with temperature	$\ln(M) \times 1/k_BT$	4	−65.7	139.8	0.16	0.13	7.8	0.009
7	r_{max} varies with adult body mass only	$\ln(M)$	2	−68	140.2	0.1	0.09	8.2	0.007
8	r_{max} varies with adult body mass and depth, and the effect of mass scaling coefficient varies with depth	$\ln(M) \times \text{depth}$	4	−66.1	140.8	0.14	0.11	8.8	0.006
9	r_{max} varies with (inverse) temperature only	$1/k_BT$	2	−69.5	143.1	0.07	0.06	11.1	0.002
10	r_{max} varies with depth only	Depth	2	−70.3	144.8	0.05	0.04	12.8	0.001
11	average r_{max} (i.e., intercept-only model)	1	1	−72.7	147.5	0	0	15.5	0

hence maximum age. Warmer temperatures and stronger predation consistently reduced cohort survival, with the strongest declines occurring in smaller offspring. Larger offspring experienced higher survival across all scenarios, especially under size-dependent predation, where size refuge substantially improved persistence yielding much greater lifespan in rays than skates (Figure 8d) than would occur with size-independent predation elevated in the tropics (Figure 8c).

Overall, the models indicate that warmer temperatures in the tropics amplify mortality risk through both metabolic and predation pathways, while both predation scenarios and larger offspring yield longer life histories in ray-like species. Nevertheless, temperature- and size-dependent predation yields much longer life histories than temperature-dependent predation alone, and hence is more likely to have driven strong selection for larger offspring and favouring life histories that reduce early-life exposure to predation in rays.

4 | Discussion

Our analyses reveal that offspring size fundamentally restructures how maximum population growth rate (r_{max}) scales with body size and temperature in rays and skates. We find that offspring size introduced an offset to the well-studied relationships of offspring size and adult mass (Figure 4a) and also between r_{max}, offspring size and temperature across 85 ray and skate species (Figure 5a). Specifically, our results show that temperature (or depth) and adult body size alone—as we previously found—do not explain as much variation in r_{max} across rays and skates (Barrowclift et al. 2023). Instead, our new analysis reveals that offspring size appears to be the key additional and primary predictor of r_{max} in these taxa, such that species (rays) with larger absolute offspring size have lower population growth rates, r_{max} (than skates). This finding helps explain the paradox of why tropical rays, which are found in warmer, shallower waters, should have higher r_{max} based on

14672979, 0, Downloaded from https://onlinelibrary.wiley.com/doi/10.1111/faf.70091 by Nick Dulvy , Wiley Online Library on [12/05/2026]. See the Terms and Conditions (https://onlinelibrary.wiley.com/terms-and-conditions) on Wiley Online Library for rules of use; OA articles are governed by the applicable Creative Commons License

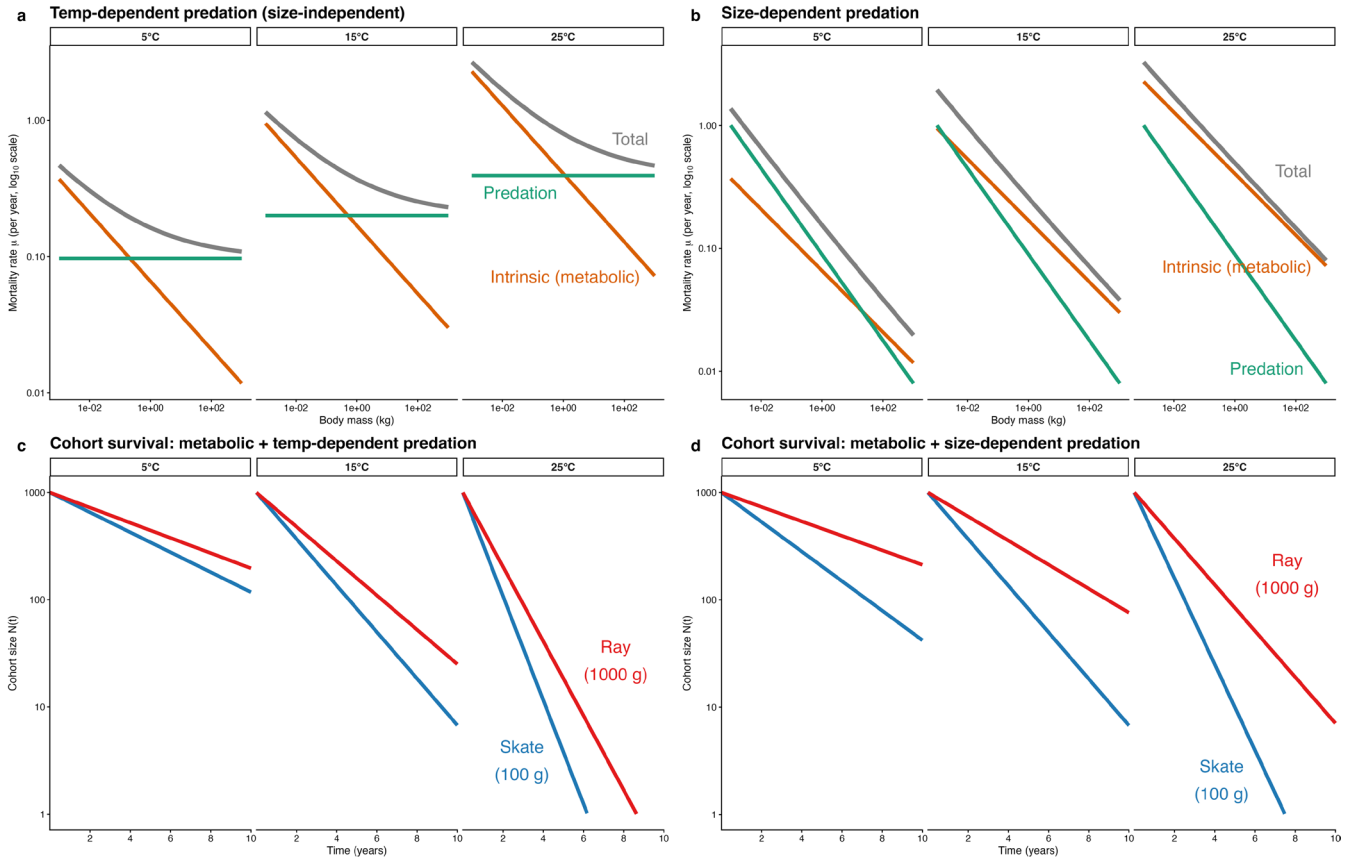

FIGURE 8 | Effects of intrinsic (metabolic) and extrinsic (predation) mortality on early-life survival (a, b) and cohort numbers (c, d). Modelled mortality rates and cohort dynamics for juvenile elasmobranchs under temperature- and size-dependent predation. (a, b) Intrinsic metabolic (orange), predation (green) and total (grey) mortality rates as functions of body mass under temperature-dependent and (a) temperature-dependent predation and (b) size-dependent predation. Corresponding cohort survival trajectories for two offspring size classes, small typical of skates (100 g, blue line) large typical of rays (1000 g, red line). Mortality scales negatively with body mass and increases with temperature following metabolic theory, while predation risk varies with either temperature or size. Larger offspring exhibit enhanced survival across scenarios more consistent with the longer lifespan of rays.

expectations from metabolic scaling theory but instead have lower population growth rates, compared to cold, deepwater skates (which have smaller offspring size). In the following six sections, we (1) examine why batoids depart from metabolic expectations; (2) demonstrate how offspring size resolves this paradox; (3) hypothesise how predation risk has shaped offspring size and reproductive strategy; (4) explore the evolutionary role of reproductive mode and predation; (5) discuss how offspring size reshapes the r_{max}–mass relationship; and (6) outline implications for conservation and management.

4.1 | Why Batoids Depart From Metabolic Expectations

Classical metabolic scaling theory predicts higher population growth rates in warmer, shallower environments, yet batoids deviate markedly from these expectations (Beukhof et al. 2019; Jennings et al. 2008; Munch and Salinas 2009). This would also lead to latitudinal and depth-related patterns of temperature and size, whereby organisms in shallower, warmer and/or lower latitude waters have higher metabolic rates and therefore 'faster' life histories compared to organisms in deeper, cooler and/or higher latitude waters (Juan-Jordá et al. 2013; Temple et al. 2020; Wong et al. 2021; Pardo and Dulvy 2022; Gravel et al. 2024). However, recent work found that compared to the cold water, deeper-dwelling skates, warm, shallow-water tropical rays have lower r_{max} and therefore greater intrinsic sensitivity to overfishing (Barrowclift et al. 2023). Consistent with previous analyses (Barrowclift et al. 2023), here we find that r_{max} increases with temperature in line with metabolic theory but has a weaker negative (adult) body mass effect in batoids than would be expected (Figure 7b).

We demonstrate that this apparent contradiction arises because offspring size modulates the scaling of r_{max} with temperature and adult body size. Specifically, offspring size and not adult size, was the most important size metric for explaining variation in r_{max} across batoid species and along with temperature or depth, explained the most variation. Generally, offspring size tends to have a negative relationship with temperature in vertebrates and invertebrates due to differences in maternal investment, with females producing larger, better-provisioned offspring in colder environments (Pettersen et al. 2020; Marshall 2021). This large-offspring-in-the-cold pattern is supported by both a cross cohort experiment of bryozoans (Marshall 2021) and a metanalysis spanning 72 species from five ectotherm phyla (Pettersen et al. 2020). However, tropical

14672979, 0, Downloaded from https://onlinelibrary.wiley.com/doi/10.1111/faf.70091 by Nick Dulvy , Wiley Online Library on [12/05/2026]. See the Terms and Conditions (https://onlinelibrary.wiley.com/terms-and-conditions) on Wiley Online Library for rules of use; OA articles are governed by the applicable Creative Commons License

rays show the converse and generally have larger offspring sizes than cooler-water-temperate skates (Figure 4a). It may be that offspring size is largely independent of temperature for batoids, with both employing very different reproductive strategies, raising the question as to why large offspring sizes have evolved in shallow-water, tropical rays. Collectively, our work suggests that at least for some taxa, the pattern of reproductive investment into offspring size is independent of (or less dependent upon) the effect temperature and size typically have on other life history traits, suggesting different selective forces operating on the evolution of offspring size.

4.2 | Offspring Size Resolves the Tropical Ray r_{max} Paradox

Our finding that offspring size explains variation in r_{max} across batoids follows from recent work suggesting that the scaling of r_{max} with adult body mass matches metabolic expectations only when offspring size is considered, and specifically, when offspring mass is proportional to adult mass (constant adult-to-offspring size ratio) (Denéchère et al. 2022). They show that across a broad swath of marine life there are two dominant life history strategies where offspring size is either proportional to adult size or invariant (uncorrelated) to adult size, with teleosts having relatively fixed invariant offspring size as an adaptation to broadcast spawning (Duarte and Alcaraz 1989), and elasmobranchs and mammals generally following the 'proportional' strategy (Neuheimer et al. 2015). For elasmobranchs, Denéchère et al. (2022) found that the scaling of r_{max} with adult mass matched metabolic expectations and that elasmobranchs had a constant adult-to-offspring size ratio (offspring size was proportional to adult size, that is, the ratio of adult size to offspring size does not increase with adult mass). We found that the ratio of adult size to offspring size was not important in the scaling of r_{max} and that in batoids, this ratio increases with adult size (i.e., it is not constant as found in Denéchère et al. (2022) when examined across a broader diversity of elasmobranchs). Further, we found that the effect size of absolute offspring mass on r_{max} was greater than that of adult mass, suggesting that offspring size limits r_{max} more strongly than adult size, and that using the ratio of adult size to offspring size had low predictive power. Offspring size, which reflects reproductive investment and life history trade-offs, greatly varied over 4.8 orders of magnitude from 0.36 g in Brown Skate (*R. miraletus*) to 26.3 kg in Oceanic Manta Ray (*M. birostris*), which may be why we were able to detect the importance of this trait in this lineage. Specifically, the differences in r_{max} between warm, shallow-water rays and cold water, deeper-dwelling skates are likely due to their different reproductive strategies—as live-bearing rays have fewer, larger offspring compared to egg-laying skates with large numbers of smaller offspring—as we speculated in Barrowclift et al. (2023).

4.3 | Predation Risk and the Evolution of Large Offspring

We hypothesise that size-based predation pressure in tropical systems has been a major selective force shaping offspring size and reproductive strategy in rays. Live-bearing has been hypothesised to have evolved from egg-laying in order to increase the survival of offspring through a controlled maternal environment and greater protection from predators (Wourms 1994; Goodwin et al. 2002). In live-bearing species, offspring size (and thus fecundity) is constrained by the size of the maternal body cavity but results in offspring with greater survival (Wourms and Lombardi 1992; Musick and Ellis 2005). Whereas in egg-laying species, size is limited by nutrients stored in the yolk sac (Carrier et al. 2004). The egg-laying reproductive strategy of skates is thought to be advantageous because it requires less energy and shorter reproductive cycles but there will be survival consequences for the offspring due to smaller size, and, thus, greater risk of predation (Goodwin et al. 2002). Consequently, there is a trade-off between the number and size of offspring resulting in a negative relationship between offspring size and annual fecundity (Smith and Fretwell 1974; Duarte and Alcaraz 1989; Cortés 2000). This was evident in our batoid dataset along with the expectation that, as for sharks, larger species tend to have larger and more offspring (Figure 4b) (Cortés 2000). Offspring size will affect juvenile survival to maturity, which is important to consider, given the maternal trade-off between lifetime reproductive output, which likely varies between egg-laying and live-bearing reproductive modes (Pardo et al. 2016). In the calculation of r_{max} for elasmobranchs, there is the pragmatic assumption that juvenile survival to maturity is the same as the survival rate of adult ages (a consistent mortality estimator). However, established size-based predation theory would suggest larger absolute offspring sizes (typical of tropical rays) would lead to lower predation risk than smaller offspring (typical of colder-water skates) (Figure 8a,c). Intrinsic (temperature-driven) combined with increased extrinsic (size-dependent) predation would lead to much greater cohort survival and much longer life histories, consistent with the vast differences in maximum age in batoids (Figure 8b,d). This then leads to the question as to why it might be advantageous for tropical, warm-water rays to have larger offspring than temperate, cold-habitat skates?

4.4 | Reproductive Mode, Predation and the Evolution of Large Offspring

Variation in offspring size and maternal investment is also linked to patterns of diversification and geographic range evolution in batoids. The ancestral reproductive mode of sharks and rays is egg-laying with the subsequent evolution of live-bearing and a particularly high degree of maternal investment found in the shallow-tropical elasmobranch species (Dulvy and Reynolds 1997; Blackburn and Hughes 2024; Mull et al. 2024). Recent work shows that the diversification and radiation of elasmobranchs throughout shallow tropical shelf seas and the pelagic zone appears to be associated with the evolution of live-bearing and multiple mechanisms for providing additional maternal investment in offspring (Mull et al. 2024). The question remains as to why live-bearing with additional maternal investment has evolved. Predation tends to be size-based in the marine realm (Verity and Smetacek 1996; Barnes et al. 2010). We hypothesise that shallow-water, tropical rays have evolved larger offspring in response to selection pressure from greater predation risk in the tropics, potentially due to the greater diversity of sharks (Dulvy et al. 2026). Increased offspring size reduces predation risk in systems structured by size-based interactions, that is, has been selected to reduce juvenile mortality

14672979, 0, Downloaded from https://onlinelibrary.wiley.com/doi/10.1111/faf.70091 by Nick Dulvy , Wiley Online Library on [12/05/2026]. See the Terms and Conditions (https://onlinelibrary.wiley.com/terms-and-conditions) on Wiley Online Library for rules of use; OA articles are governed by the applicable Creative Commons License

(Figure 8d) (Cortés 2000; Olsson et al. 2016; Sibly et al. 2018). We hypothesise that this size-based predation risk drove the evolution of live-bearing, and in particular the convergent evolution of multiple forms of matrotrophy (maternal supply of nutrients during gestation), in order to yield larger offspring. Olsson et al. (2016) proposed that the optimal offspring size strategy (either invariant or proportional to adult size) depends on the life stage where density-dependence occurs, with the invariant strategy associated with an absence of density-dependence in early life and a proportional strategy being subject to density-dependence throughout life. This hypothesis aligns with proposed higher predation selection for larger offspring size in tropical rays as density-dependence would become more important in later life history stages where survival is less constrained by predation. We find that size-based predation (proportional) and larger offspring sizes is more likely to yield the longer life histories of rays compared to the invariant strategy (Figure 8a,c vs. Figure 8b,d). Generally, offspring size is larger in chondrichthyans compared to teleost fishes in which live-bearing appears to have evolved in particularly small-bodied taxa, suggesting the drivers of viviparity are fundamentally different in chondrichthyans (Goodwin et al. 2002). Predation risk has generally been hypothesised to increase towards the tropics, with recent empirical work finding greater predation rates on epifaunal communities in shallow, tropical waters compared to high latitude waters (Ashton et al. 2022). This is relevant to potential greater predation on eggs and juveniles in tropical waters. Fisheries-driven decline in sharks (which predate on batoids) has led to increases in ray abundance, consistent with our hypothesis that predation is a major evolutionary force in tropical systems (Sherman et al. 2020; Simpfendorfer et al. 2023).

4.5 | How Offspring Size Reshapes the r_{max}-Mass Relationship

Given the TSR, adult body size of temperate skates in cooler waters would be expected to be larger than tropical rays in warmer waters. However, our results suggest there is wide variation in adult body size across batoids and, generally, the tropical rays are larger than cooler-water skates, ranging from 516 g in Spinytail Round Ray (*Urotrygon aspidura*) to 3000 kg in the Oceanic Manta Ray. We hypothesise above that the larger offspring sizes and live-bearing are a result of elevated predation in the tropics; given the body cavity constraint on offspring size of live-bearers we further speculate that large offspring size would require the evolution of larger adult body sizes in tropical rays that would allow greater maternal investment. This is consistent with the adult body size differences being the opposite of what might be expected under a TSR hypothesis, that is, larger in tropical rays and smaller in cool-water skates, and may explain this exception to the TSR where tropical rays attain larger sizes at higher temperatures (Atkinson 1995). Instead, our findings are more consistent with a mortality theory of life histories, and specifically the mortality arising from predation risk and offspring size (Auer et al. 2018; Glazier 2023).

The evolution of maternal investment (and hence larger than expected offspring size) as discussed above seems associated with greater maternal size (and hence larger offspring size), for example gigantism in manta and devil rays (*Mobula* spp.) and greater diversification (speciation minus extinction) in tropical elasmobranchs (Mull et al. 2024). Although we also note elevated diversification in skates, which is hypothesised to be due to a different mechanism, resulting from the opening of the Atlantic Ocean and creation of a large expanse of shallow temperate and deepwater habitats that were rapidly colonised by skates (Mull et al. 2024). Due to their low egg and adult dispersal capability, skates tend to speciate with increasing geographic separation as they do not seem able to transit deepwater channels that would have appeared between island chains and continental shelves as the Atlantic Ocean opened and hence have smaller geographic ranges than live-bearers (McEachran and Miyake 1990; Long 1994; Goodwin et al. 2005). For example, there is a high richness of skates in South America, South Africa and Australia, areas that were formerly connected as part of Gondwanaland, and have now evolved distinct faunas (Last and Yearsley 2002; Figueroa et al. 2023). It would be interesting to explore a relationship between areas of high species richness and the offspring size strategy employed.

4.6 | Macroevolutionary and Conservation Implications

We found that offspring size, alongside temperature or depth, explained variation in r_{max} for rays and skates rather than adult body size or the adult-to-offspring size ratio. Offspring size reflects maternal energy investment that is part of a key trade-off between reproduction, growth and survival. Offspring size has direct fitness consequences through the allocation of resources provisioned to offspring for growth, survival and reproductive success, and therefore has ecological and evolutionary implications (Pettersen et al. 2022) and as we show here variation in r_{max} (Figure 7). One possible explanation for the weaker adult body size effect observed than would be predicted by metabolic theory is that body size influences r_{max} through multiple pathways. This includes a direct physiological pathway through metabolic rate (faster life histories in warmer temperatures, grow faster to a smaller maximum body size, higher r_{max}) but also through the indirect pathway of life history selection on offspring size, mediated by typically size-based predation risk (Figure 8b,d). Our results suggest that offspring size may partially offset the direct metabolic scaling of adult body size on r_{max}, particularly across different temperatures (Figure 8c,d).

We highlight five research directions. (1) Future research would likely benefit from a causal modelling approach to estimate the relative strength of these different pathways and how this affects species and population productivity. (2) Given the strong phylogenetic signal in the r_{max} residuals, it is likely that maximum population growth rate is shaped by biological traits that are evolutionarily conserved, which would allow for predictive modelling of r_{max} based on phylogenetic relationships (Pardo and Dulvy 2022; Horswill et al. 2025; Dulvy et al. 2026). (3) Additional variation in r_{max} that was not explained by our models may be explained by further environmental and physiological variables such as dissolved oxygen or metabolic rate (Pardo and Dulvy 2022; Gravel et al. 2024) or plasticity in life history traits driven by energy availability (Lucas et al. 2025). Indeed, further understanding of the relationship between offspring size and metabolic rate is needed (Pettersen et al. 2022). (4) Empirical estimates of juvenile mortality for sharks and rays

14672979, 0, Downloaded from https://onlinelibrary.wiley.com/doi/10.1111/faf.70091 by Nick Dulvy , Wiley Online Library on [12/05/2026]. See the Terms and Conditions (https://onlinelibrary.wiley.com/terms-and-conditions) on Wiley Online Library for rules of use; OA articles are governed by the applicable Creative Commons License

are still required to better understand juvenile survival across species with different life history strategies (incorporating how growth and mortality vary with body size). Whilst the mortality estimator used in the modified Euler-Lotka model to calculate r_{max} accounts for juvenile survival to maturity, there is a need for the development of size-dependent mortality rates to investigate differences across reproductive and offspring size strategies. Extending analyses across sharks would also allow testing whether the relationships identified between maximum population growth rate and mortality patterns identified in batoids represent broader demographic patterns across elasmobranchs. (5) We offer a basic modelling framework to illustrate our mortality hypothesis but encourage a deeper analysis of Evolutionary Stable Strategies or through state-dependent approaches (Olsson et al. 2016). Although the broad biogeographic separation between rays and skates is evident in our results, our dataset also highlights a small number of exceptions to this pattern (skates inhabiting shallow, tropical waters and deep, cooler-water rays) that warrant further exploration of the drivers of selection on offspring size. For example, extended or continuous egg-laying periods to increase fecundity in warm-water skates due to higher juvenile mortality from increased predation than similar temperate-water species.

Our results suggest that these differences may be key to understanding biogeographic patterns in extinction risk. We posit that greater predation risk in the tropics has driven the evolution of larger offspring size to increase offspring survival in tropical rays, potentially through live-bearing reproductive mode, increased matrotrophy, and larger adult body sizes. Consequently, shallow-water tropical rays have lower r_{max} and therefore limited capacity to compensate for fishing mortality, making them more intrinsically sensitive to overfishing and slower to recover than may be expected from metabolic ecology alone. This research agenda will provide the capacity to develop clade-wide predictions of r_{max} essential to support the development of proposals to regulate the international trade in skate meat and ray skins and support national development of sustainable fisheries and CITES non-detriment findings (MacNeil et al. 2025; Dulvy et al. 2026).

Author Contributions

Ellen Barrowclift: conceptualisation, methodology, formal analysis, investigation, validation, data curation, writing – original draft preparation, writing – review and editing, visualisation, funding acquisition. **Jennifer S. Bigman:** formal analysis, writing – reviewing and editing. **Eric D. Digel:** formal analysis, writing – reviewing and editing. **Per Berggren:** writing – reviewing and editing, supervision, funding acquisition. **Nicholas K. Dulvy:** conceptualisation, methodology, formal analysis, investigation, validation, data curation, writing – original draft preparation, writing – review and editing, visualisation, funding acquisition, supervision.

Acknowledgements

E.B. was funded by a Natural Environment Research Council (NERC) PhD studentship through the IAPETUS2 Doctoral Training Partnership (award ref. 2284959) and a UK Research and Innovation (UKRI)-Mitacs UK-Canada Globalink Research Placement (award ref. NE/T014555/1). J.S.B. was supported by the National Science Foundation (NSF grant number 2109411). N.K.D. was supported by the Natural Sciences and Engineering Research Council of Canada Discovery and Accelerator Awards (grant numbers 5013566 and 462291) and the Canada Research Chairs program (grant number 1228186).

Conflicts of Interest

The authors declare no conflicts of interest.

Data Availability Statement

The datasets supporting this article are available at FigShare (DOI: https://doi.org/10.6084/m9.figshare.20182109). The R code to reproduce these analyses will be available at Github (https://github.com/EBarrowclift/batoid-rmax-offspring-scaling).

References

Arnold, T. W. 2010. "Uninformative Parameters and Model Selection Using Akaike's Information Criterion." *Journal of Wildlife Management* 74, no. 6: 1175–1178. https://doi.org/10.1111/j.1937-2817.2010.tb01236.x.

Ashton, G. V., A. L. Freestone, J. E. Duffy, et al. 2022. "Predator Control of Marine Communities Increases With Temperature Across 115 Degrees of Latitude." *Science* 376, no. 6598: 1215–1219. https://doi.org/10.1126/science.abc4916.

Atkinson, D. 1994. "Temperature and Organism Size—A Biological Law for Ectotherms?" *Advances in Ecological Research* 25, no. C: 1–58. https://doi.org/10.1016/S0065-2504(08)60212-3.

Atkinson, D. 1995. "Effects of Temperature on the Size of Aquatic Ectotherms: Exceptions to the General Rule." *Journal of Thermal Biology* 20, no. 1–2: 61–74. https://doi.org/10.1016/0306-4565(94)00028-H.

Atkinson, D., S. A. Morley, and R. N. Hughes. 2006. "From Cells to Colonies: At What Levels of Body Organization Does the "Temperature-Size Rule" Apply?" *Evolution & Development* 8, no. 2: 202–214. https://doi.org/10.1111/J.1525-142X.2006.00090.X.

Atkinson, D., and R. M. Sibly. 1997. "Why Are Organisms Usually Bigger in Colder Environments? Making Sense of a Life History Puzzle." *Trends in Ecology & Evolution* 12, no. 6: 235–239. https://doi.org/10.1016/S0169-5347(97)01058-6.

Auer, S. K., C. A. Dick, N. B. Metcalfe, and D. N. Reznick. 2018. "Metabolic Rate Evolves Rapidly and in Parallel With the Pace of Life History." *Nature Communications* 9, no. 14: 6. https://doi.org/10.1038/s41467-017-02514-z.

Barnes, C., D. Maxwell, D. C. Reuman, and S. Jennings. 2010. "Global Patterns in Predator-Prey Size Relationships Reveal Size Dependency of Trophic Transfer Efficiency." *Ecology* 91, no. 1: 222–232. https://doi.org/10.1890/08-2061.1.

Barrowclift, E., and N. K. Dulvy. 2023. "Life History and Maximum Weight Database for Rays (Class Chondrichthyes, Superorder Batoidea) up to June 2022." Figshare. https://doi.org/10.6084/m9.figshare.20182109.v3.

Barrowclift, E., S. M. Gravel, S. A. Pardo, J. S. Bigman, P. Berggren, and N. K. Dulvy. 2023. "Tropical Rays Are Intrinsically More Sensitive to Overfishing Than the Temperate Skates." *Biological Conservation* 281: 110003. https://doi.org/10.1016/j.biocon.2023.110003.

Bernhardt, J. R., J. M. Sunday, and M. I. O'Connor. 2018. "Metabolic Theory and the Temperature-Size Rule Explain the Temperature Dependence of Population Carrying Capacity." *American Naturalist* 192, no. 6: 687–697. https://doi.org/10.1086/700114.

Beukhof, E., R. Frelat, L. Pecuchet, et al. 2019. "Marine Fish Traits Follow Fast-Slow Continuum Across Oceans." *Scientific Reports* 9, no. 1: 17878. https://doi.org/10.1038/S41598-019-53998-2.

14672979, 0, Downloaded from https://onlinelibrary.wiley.com/doi/10.1111/faf.70091 by Nick Dulvy , Wiley Online Library on [12/05/2026]. See the Terms and Conditions (https://onlinelibrary.wiley.com/terms-and-conditions) on Wiley Online Library for rules of use; OA articles are governed by the applicable Creative Commons License

Blackburn, D. G., and D. F. Hughes. 2024. "Phylogenetic Analysis of Viviparity, Matrotrophy, and Other Reproductive Patterns in Chondrichthyan Fishes." *Biological Reviews* 99, no. 4: 1314–1356. https://doi.org/10.1111/BRV.13070.

Boettiger, C., D. T. Lang, and P. C. Wainwright. 2012. "Rfishbase: Exploring, Manipulating and Visualizing FishBase Data From R." *Journal of Fish Biology* 81, no. 6: 2030–2039. https://doi.org/10.1111/J.1095-8649.2012.03464.X.

Brown, J. H., J. F. Gillooly, A. P. Allen, V. M. Savage, and G. B. West. 2004. "Toward a Metabolic Theory of Ecology." *Ecology* 85, no. 7: 1771–1789. https://doi.org/10.1890/03-9000.

Burger, J. R., C. Hou, and J. H. Brown. 2019. "Toward a Metabolic Theory of Life History." *Proceedings of the National Academy of Sciences of the United States of America* 116, no. 52: 26653–26661. https://doi.org/10.1073/PNAS.1907702116/SUPPL_FILE/PNAS.1907702116.SAPP.PDF.

Burnham, K. P., and D. R. Anderson. 2002. *Model Selection and Multimodel Inference: A Practical Information-Theoretic Approach*. 2nd ed. Springer. https://doi.org/10.1007/b97636.

Carrier, J. C., H. L. Pratt, and J. I. Castro. 2004. "Reproductive Biology of Elasmobranchs." In *Biology of Sharks and Their Relatives*, edited by J. C. Carrier, J. A. Musick, and M. R. Heithaus, 1th ed., 269–286. CRC Press.

Cortés, E. 2000. "Life History Patterns and Correlations in Sharks." *Reviews in Fisheries Science* 8, no. 4: 299–344. https://doi.org/10.1080/10408340308951115.

Cortés, E. 2016. "Perspectives on the Intrinsic Rate of Population Growth." *Methods in Ecology and Evolution* Edited by J. Travis 7, no. 10: 1136–1145. https://doi.org/10.1111/2041-210x.12592.

Denéchère, R., P. D. van Denderen, and K. H. Andersen. 2022. "Deriving Population Scaling Rules From Individual-Level Metabolism and Life History Traits." *American Naturalist* 199, no. 4: 564–575. https://doi.org/10.1086/718642.

Duarte, C. M., and M. Alcaraz. 1989. "To Produce Many Small or Few Large Eggs: A Size-Independent Reproductive Tactic of Fish." *Oecologia* 80, no. 3: 401–404. https://doi.org/10.1007/bf00379043.

Dulvy, N. K., R. Aitchison, A. Arnold, et al. 2026. "Bending Back the Curve of Shark and Ray Biodiversity Loss." *Nature Reviews Biodiversity* 2: 92–115. https://doi.org/10.1038/s44358-025-00120-2.

Dulvy, N. K., J. R. Ellis, N. B. Goodwin, A. Grant, J. D. Reynolds, and S. Jennings. 2004. "Methods of Assessing Extinction Risk in Marine Fishes." *Fish and Fisheries* 5, no. 3: 255–276. https://doi.org/10.1111/j.1467-2679.2004.00158.x.

Dulvy, N. K., S. L. Fowler, J. A. Musick, et al. 2014. "Extinction Risk and Conservation of the World's Sharks and Rays." *eLife* 3: 590. https://doi.org/10.7554/eLife.00590.

Dulvy, N. K., N. Pacoureau, C. L. Rigby, et al. 2021. "Overfishing Drives Over One-Third of All Sharks and Rays Toward a Global Extinction Crisis." *Current Biology* 31, no. 21: 4773–4787. https://doi.org/10.1016/j.cub.2021.08.062.

Dulvy, N. K., and J. Reynolds. 1997. "Evolutionary Transitions Among Egg-Laying, Live-Bearing and Maternal Inputs in Sharks and Rays." *Proceedings of the Royal Society of London. Series B, Biological Sciences* 264: 1309–1315.

Ebert, D. A., and L. J. V. Compagno. 2007. "Biodiversity and Systematics of Skates (Chondrichthyes: Rajiformes: Rajoidei)." *Environmental Biology of Fishes* 80, no. 2–3: 111–124. https://doi.org/10.1007/S10641-007-9247-0/FIGURES/5.

Figueroa, D. E., S. A. Barbini, M. Belleggia, D. E. Sabadin, J. M. Román, and A. M. De Wysiecki. 2023. "The Ichthyofaunistic Colonization and Complex Biogeographic History of the Southern Portion of the Southwest Atlantic Ocean." *Marine Ecology* 44, no. 2: e12742. https://doi.org/10.1111/MAEC.12742.

Fox, J., and S. Weisberg. 2019. *An R Companion to Applied Regression*. 3rd ed. Sage. https://socialsciences.mcmaster.ca/jfox/Books/Companion/.

Frisk, M. 2010. "Life History Strategies of Batoids." In *Sharks and Their Relatives II: Biodiversity, Adaptive Physiology, and Conservation*, edited by C. Carrier, J. A. Musick, and M. R. Heithaus, 283–316. CRC Press. https://doi.org/10.1201/9781420080483-c6.

Froese, R., and D. Pauly. 2022. "FishBase. World Wide Web Electronic Publication." https://www.fishbase.org.

Glazier, D. S. 2023. "The Relevance of Time in Biological Scaling." *Biology* 12: 1084. https://doi.org/10.3390/biology12081084.

Goodwin, N. B., N. K. Dulvy, and J. D. Reynolds. 2002. "Life-History Correlates of the Evolution of Live Bearing in Fishes." *Philosophical Transactions of the Royal Society of London. Series B, Biological Sciences* 357: 259–267. https://doi.org/10.1098/rstb.2001.0958.

Goodwin, N. B., N. K. Dulvy, and J. D. Reynolds. 2005. "Macroecology of Live-Bearing in Fishes: Latitudinal and Depth Range Comparisons With Egg-Laying Relatives." *Oikos* 110, no. 2: 209–218. https://doi.org/10.1111/J.0030-1299.2005.13859.X.

Gravel, S., J. S. Bigman, S. A. Pardo, S. Wong, and N. K. Dulvy. 2024. "Metabolism, Population Growth, and the Fast-Slow Life History Continuum of Marine Fishes." *Fish and Fisheries* 25: 349–361. https://doi.org/10.1111/faf.12811.

Horswill, C., H. K. Kindsvater, N. K. Dulvy, et al. 2025. "Imputation of Fisheries Reference Points for Endangered Data-Poor Fishes, With Application to Rhino Rays." *Fish and Fisheries* 26: 848–865. https://doi.org/10.1111/faf.70003.

Hutchings, J. A., R. A. Myers, V. B. García, L. O. Lucifora, and A. Kuparinen. 2012. "Life-History Correlates of Extinction Risk and Recovery Potential." *Ecological Applications* 22, no. 4: 1061–1067. https://doi.org/10.1890/11-1313.1.

Jennings, S., F. Mélin, J. L. Blanchard, R. M. Forster, N. K. Dulvy, and R. W. Wilson. 2008. "Global-Scale Predictions of Community and Ecosystem Properties From Simple Ecological Theory." *Proceedings of the Royal Society B: Biological Sciences* 275, no. 1641: 1375–1383. https://doi.org/10.1098/RSPB.2008.0192.

Juan-Jordá, M. J., I. Mosqueira, A. B. Cooper, J. Freire, and N. K. Dulvy. 2011. "Global Population Trajectories of Tunas and Their Relatives." *Proceedings of the National Academy of Sciences of the United States of America* 108, no. 51: 20650–20655. https://doi.org/10.1073/PNAS.1107743108.

Juan-Jordá, M. J., I. Mosqueira, J. Freire, and N. K. Dulvy. 2013. "Life in 3-D: Life History Strategies in Tunas, Mackerels and Bonitos." *Reviews in Fish Biology and Fisheries* 23, no. 2: 135–155. https://doi.org/10.1007/S11160-012-9284-4/FIGURES/4.

Juan-Jordá, M. J., I. Mosqueira, J. Freire, and N. K. Dulvy. 2015. "Population Declines of Tuna and Relatives Depend on Their Speed of Life." *Proceedings of the Royal Society B, Biological Sciences* 282, no. 1811: 20150322. https://doi.org/10.1098/rspb.2015.0322.

Last, P. R., W. T. White, M. R. de Carvalho, B. Séret, M. F. W. Stehmann, and G. J. P. Naylor. 2016. *Rays of the World*. CSIRO Publishing.

Last, P. R., and G. K. Yearsley. 2002. "Zoogeography and Relationships of Australasian Skates (Chondrichthyes: Rajidae)." *Journal of Biogeography* 29, no. 12: 1627–1641. https://doi.org/10.1046/J.1365-2699.2002.00793.X.

Long, D. J. 1994. "Quaternary Colonization or Paleogene Persistence?: Historical Biogeography of Skates (Chondrichthyes: Rajidae) in the Antarctic Ichthyofauna." *Paleobiology* 20, no. 2: 215–228. https://doi.org/10.1017/S0094837300012690.

14672979, 0, Downloaded from https://onlinelibrary.wiley.com/doi/10.1111/faf.70091 by Nick Dulvy , Wiley Online Library on [12/05/2026]. See the Terms and Conditions (https://onlinelibrary.wiley.com/terms-and-conditions) on Wiley Online Library for rules of use; OA articles are governed by the applicable Creative Commons License

Lucas, S., P. Berggren, E. Barrowclift, and I. M. Smallegange. 2025. "Changing Feeding Levels Reveal Plasticity in Elasmobranch Life History Strategies." *Ecology Letters* 28, no. 9: e70201. https://doi.org/10.1111/ele.70201.

Luhring, T. M., and J. P. Delong. 2017. "Scaling From Metabolism to Population Growth Rate to Understand How Acclimation Temperature Alters Thermal Performance." *Integrative and Comparative Biology* 57, no. 1: 103–111. https://doi.org/10.1093/icb/icx041.

MacNeil, M. A., C. Mull, A. Martins, et al. 2025. "Hidden Diversity of Threatened Sharks and Rays in the Global Meat Trade." bioRxiv, 34, p. 2025.04.24.650194. https://doi.org/10.1101/2025.04.24.650194.

Marshall, D. J. 2021. "Temperature-Mediated Variation in Selection on Offspring Size: A Multi-Cohort Field Study." *Functional Ecology* 35, no. 10: 2219–2228. https://doi.org/10.1111/1365-2435.13879.

McEachran, J., and T. Miyake. 1990. "Zoogeography and Bathymetry of Skates (Chondrichthyes, Rajoidei)." In *Elasmobranchs as Living Resources: Advances in the Biology, Ecology, Systematics, and the Status of the Fisheries*, edited by H. L. Pratt, S. H. Gruber, and T. Taniuchi, 90. NOAA Technical Report National Marine Fisheries Service. https://www.semanticscholar.org/paper/Elasmobranchs-as-living-resources%3A-advances-in-the-Pratt-Gruber/b36e50b41efa176f12b596aa9ff55da8bbe5daef.

Mejía, D., C. Robalino-Mejía, F. Galván-Magaña, et al. 2025. "A Global Synthesis of Population Demographic Models in Sharks and Rays." *Fish and Fisheries* 26, no. 4: 587–602. https://doi.org/10.1111/FAF.12900.

Moro, S., S. Valente, M. Arcioni, et al. 2025. "Living on the Extinction Edge: Resilience to Fishing and Rebound Potential of the Mediterranean Elasmobranchs." *Fish and Fisheries* 26: 772–789. https://doi.org/10.1111/FAF.12911.

Mull, C., N. Pacoureau, S. A. Pardo, et al. 2022. "Sharkipedia: A Curated Open-Access Database of Shark and Ray Life History Traits and Abundance Time-Series." *Scientific Data* 9, no. 1: 559. https://doi.org/10.1038/s41597-022-01655-1.

Mull, C. G., M. W. Pennell, K. E. Yopak, and N. K. Dulvy. 2024. "Maternal Investment Evolves With Larger Body Size and Higher Diversification Rate in Sharks and Rays." *Current Biology* 34, no. 12: 2773–2781. https://doi.org/10.1016/j.cub.2024.05.019.

Munch, S. B., and S. Salinas. 2009. "Latitudinal Variation in Lifespan Within Species is Explained by the Metabolic Theory of Ecology." *Proceedings of the National Academy of Sciences of the United States of Amercia* 106, no. 33: 13860–13864. https://doi.org/10.1073/pnas.0900300106.

Musick, J. A., and J. K. Ellis. 2005. "Reproductive Evolution of Chondrichthyans." In *Reproductive Biology and Phylogeny of Chondrichthyes*, edited by W. C. Hamlett, 1st ed., 45–78. CRC press.

Myers, R. A., G. Mertz, and P. S. Fowlow. 1997. "Maximum Population Growth Rates and Recovery Times for Atlantic Cod, *Gadus morhua*." *Fishery Bulletin* 95: 762–772.

Myers, R. A., and B. Worm. 2005. "Extinction, Survival or Recovery of Large Predatory Fishes." *Philosophical Transactions of the Royal Society of London. Series B, Biological Sciences* 360, no. 1453: 13–20. https://doi.org/10.1098/RSTB.2004.1573.

Neuheimer, A. B., M. Hartvig, J. Heuschele, et al. 2015. "Adult and Offspring Size in the Ocean Over 17 Orders of Magnitude Follows Two Life History Strategies." *Ecology* 96, no. 12: 3303–3311. https://doi.org/10.1890/14-2491.1.

Olsson, K. H., H. Gislason, and K. H. Andersen. 2016. "Differences in Density-Dependence Drive Dual Offspring Size Strategies in Fish." *Journal of Theoretical Biology* 407: 118–127. https://doi.org/10.1016/J.JTBI.2016.07.027.

Orme, D., R. Freckleton, G. Thomas, et al. 2018. "Caper: Comparative Analyses of Phylogenetics and Evolution in R." https://cran.r-project.org/package=caper.

Pardo, S. A., and N. K. Dulvy. 2022. "Body Mass, Temperature, and Depth Shape the Maximum Intrinsic Rate of Population Increase in Sharks and Rays." *Ecology and Evolution* 12: e9441. https://doi.org/10.1002/ece3.9441.

Pardo, S. A., H. K. Kindsvater, J. D. Reynolds, and N. K. Dulvy. 2016. "Maximum Intrinsic Rate of Population Increase in Sharks, Rays, and Chimaeras: The Importance of Survival to Maturity." *Canadian Journal of Fisheries and Aquatic Sciences* 73, no. 8: 1159–1163. https://doi.org/10.1139/cjfas-2016-0069.

Pettersen, A. K., L. Schuster, and N. B. Metcalfe. 2022. "The Evolution of Offspring Size: A Metabolic Scaling Perspective." *Integrative and Comparative Biology* 62, no. 5: 1492–1502. https://doi.org/10.1093/ICB/ICAC076.

Pettersen, A. K., C. R. White, R. J. Bryson-Richardson, and D. J. Marshall. 2020. "Linking Life-History Theory and Metabolic Theory Explains the Offspring Size-Temperature Relationship." *Ecology Letters* 22, no. 3: 518–526. https://doi.org/10.1111/ele.13213.

R Core Team. 2021. *R: A Language and Environment for Statistical Computing*. R Foundation for Statistical Computing. https://www.r-project.org/.

RStudio Team. 2021. *RStudio: Integrated Development Environment for R*. RStudio, PBC. http://www.rstudio.com/.

Savage, V. M., J. F. Gillooly, J. H. Brown, G. B. West, and E. L. Charnov. 2004. "Effects of Body Size and Temperature on Population Growth." *American Naturalist* 163, no. 3: 429–441. https://doi.org/10.1086/381872.

Sherman, S. C., C. S. Sherman, M. R. Heupel, S. K. Moore, A. Chin, and C. A. Simpfendorfer. 2020. "When Sharks Are Away, Rays Will Play: Effects of Top Predator Removal in Coral Reef Ecosystems." *Marine Ecology Progress Series* 641: 145–157. https://doi.org/10.3354/meps13307.

Sibly, R. M., A. Kodric-Brown, S. M. Luna, and J. H. Brown. 2018. "The Shark-Tuna Dichotomy: Why Tuna Lay Tiny Eggs but Sharks Produce Large Offspring." *Royal Society Open Science* 5, no. 8: 180453. https://doi.org/10.1098/RSOS.180453.

Simpfendorfer, C. A., M. R. Heithaus, M. R. Heupel, et al. 2023. "Widespread Diversity Deficits of Coral Reef Sharks and Rays." *Science* 380, no. 6650: 1155–1160. https://doi.org/10.1126/science.ade4884.

Smith, C. C., and S. D. Fretwell. 1974. "The Optimal Balance Between Size and Number of Offspring." *American Naturalist* 108, no. 962: 499–506. https://doi.org/10.1086/282929.

Stein, R. W., C. G. Mull, T. S. Kuhn, et al. 2018. "Global Priorities for Conserving the Evolutionary History of Sharks, Rays and Chimaeras." *Nature Ecology & Evolution* 2, no. 2: 288–298. https://doi.org/10.1038/s41559-017-0448-4.

Temple, A. J., S. M. Stead, N. Jiddawi, et al. 2020. "Life-History, Exploitation and Extinction Risk of the Data-Poor Baraka's Whipray (*Maculabatis ambigua*) in Small-Scale Tropical Fisheries." *Journal of Fish Biology* 97: 708–719. https://doi.org/10.1111/jfb.14425.

Thorson, J. T. 2020. "Predicting Recruitment Density Dependence and Intrinsic Growth Rate for All Fishes Worldwide Using a Data-Integrated Life-History Model." *Fish and Fisheries* 21, no. 2: 237–251. https://doi.org/10.1111/FAF.12427.

Verity, P. G., and V. Smetacek. 1996. "Organism Life Cycles, Predation, and the Structure of Marine Pelagic Ecosystems." *Marine Ecology Progress Series* 130: 277–293.

14672979, 0, Downloaded from https://onlinelibrary.wiley.com/doi/10.1111/faf.70091 by Nick Dulvy , Wiley Online Library on [12/05/2026]. See the Terms and Conditions (https://onlinelibrary.wiley.com/terms-and-conditions) on Wiley Online Library for rules of use; OA articles are governed by the applicable Creative Commons License

Wong, S., J. S. Bigman, and N. K. Dulvy. 2021. "The Metabolic Pace of Life Histories Across Fishes." *Proceedings of the Royal Society B: Biological Sciences* 288, no. 1953: 20210910. https://doi.org/10.1098/rspb.2021.0910.

Worm, B., B. Davis, L. Kettemer, et al. 2013. "Global Catches, Exploitation Rates, and Rebuilding Options for Sharks." *Marine Policy* 40, no. 1: 194–204. https://doi.org/10.1016/J.MARPOL.2012.12.034.

Wourms, J. P. 1994. "The Challenges of Piscine Viviparity." *Israel Journal of Ecology & Evolution* 40, no. 3–4: 551–568. https://doi.org/10.1080/00212210.1994.10688772.

Wourms, J. P., and J. Lombardi. 1992. "Reflections on the Evolution of Piscine Viviparity." *American Zoologist* 32, no. 2: 276–293. https://doi.org/10.1093/icb/32.2.276.

Supporting Information

Additional supporting information can be found online in the Supporting Information section. **Table S1:** All 32 models tested with associated hypotheses for how maximum intrinsic rate of population increase (r_{max}) varies with adult body mass M, offspring body mass $M_{offspring}$, inverse temperature $1/k_BT$, depth, and a temperature-depth index (PC1 axis from Principle Components Analysis of collapsed temperature and depth data in Barrowclift et al. (2023)). Comparison of 32 $\ln(r_{max})$ models using corrected Akaike Information Criteria (AICc), number of parameters (n), negative log-likelihood (−LL), R^2, adjusted R^2 (Adj. R^2), difference in AICc from the top model (ΔAICc), and Akaike weights. Models are ordered by ascending AICc, with models with AICc < 2 shown in bold. Note, Order was categorical for rays (Orders Myliobatiformes, Rhinopristiformes and Torpediniformes) and skates (Order Rajiformes). **Table S2:** Sensitivity test for the choice of phylogenetic tree. Comparison of 11 $\ln(r_{max})$ models fitted with 10 different phylogenetic trees obtained from Stein et al. (2018) (available on Vertlife.org) using corrected Akaike Information Criteria (AICc). The model with lowest AICc for each iteration is shown in bold. **Table S3:** Sensitivity test for the exclusion of manta rays. Comparison of 11 $\ln(r_{max})$ models fitted without data for two manta ray species (*Mobula alfredi* and *M. birostris*) with largest offspring sizes using corrected Akaike Information Criteria (AICc), number of parameters (n), negative log-likelihood (−LL), R^2, adjusted R^2 (Adj. R^2), difference in AICc from the top model (ΔAICc), and Akaike weights. Models are ordered by ascending AICc and models with AICc < 2 shown in bold. **Table S4:** Coefficient estimates (95% confidence intervals estimated from standard errors shown in brackets) for all 11 models of $\ln(r_{max})$. Models are ordered by ascending AICc, with models with ΔAICc < 2 shown in bold. Pagel's λ indicates the strength of the phylogenetic signal. **Figure S1:** (a, c) Species richness with latitude for skates (a; $n = 284$ species of Rajiformes) and rays (c; $n = 339$ species of Torpediniformes, Rhinopristiformes and Myliobatiformes). The lines on the plots in the left panel are a loess (locally weighted regression) smooth fitted to the upper 10th centile of data with a span of 0.4. (b, d) Density of data points for skates (b) and rays (d). **Figure S2:** Phylogeny, maximum intrinsic rate of population increase (r_{max}), adult and offspring mass (g), offspring to adult size ratio, depth (m) and temperature (°C) in log10 space for 85 rays ($n = 53$, red points) and skates ($n = 32$, blue points). Solid lines show median values. Uncertainty in r_{max} estimate shown with 2.5% and 97.5% quantiles. Phylogenetic tree from Stein et al. (2018) (available on Vertlife.org) with binomial nomenclature updated to reflect current taxonomic nomenclature.

14672979, 0, Downloaded from https://onlinelibrary.wiley.com/doi/10.1111/faf.70091 by Nick Dulvy , Wiley Online Library on [12/05/2026]. See the Terms and Conditions (https://onlinelibrary.wiley.com/terms-and-conditions) on Wiley Online Library for rules of use; OA articles are governed by the applicable Creative Commons License